

Article

Flux Enforcement for Fermentative Production of 5-Aminovalerate and Glutarate by *Corynebacterium glutamicum*

Carsten Haupka ¹, Baudoin Delépine ², Marta Irla ³, Stephanie Heux ²
and Volker F. Wendisch ^{1,*}

¹ Genetics of Prokaryotes, Faculty of Biology and CeBiTec, Bielefeld University, Universitätsstr. 25, 33615 Bielefeld, Germany; chaupka@cebitec.uni-bielefeld.de

² TBI, Université de Toulouse, CNRS, INRAE, INSA, 31077 Toulouse, France; baudoin.delepine@inrae.fr (B.D.); heux@insa-toulouse.fr (S.H.)

³ Department of Biotechnology and Food Science, Norwegian University of Science and Technology (NTNU), 7034 Trondheim, Norway; marta.k.irla@ntnu.no

* Correspondence: volker.wendisch@uni-bielefeld.de

Received: 28 August 2020; Accepted: 14 September 2020; Published: 16 September 2020



Abstract: Bio-based plastics represent an increasing percentage of the plastics economy. The fermentative production of bioplastic monomer 5-aminovalerate (5AVA), which can be converted to polyamide 5 (PA 5), has been established in *Corynebacterium glutamicum* via two metabolic pathways. L-lysine can be converted to 5AVA by either oxidative decarboxylation and subsequent oxidative deamination or by decarboxylation to cadaverine followed by transamination and oxidation. Here, a new three-step pathway was established by using the monooxygenase putrescine oxidase (Puo), which catalyzes the oxidative deamination of cadaverine, instead of cadaverine transaminase. When the conversion of 5AVA to glutarate was eliminated and oxygen supply improved, a 5AVA titer of 3.7 ± 0.4 g/L was reached in microcultivation that was lower than when cadaverine transaminase was used. The elongation of the new pathway by 5AVA transamination by GABA/5AVA aminotransferase (GabT) and oxidation by succinate/glutarate semialdehyde dehydrogenase (GabD) allowed for glutarate production. Flux enforcement by the disruption of the L-glutamic acid dehydrogenase-encoding gene *gdh* rendered a single transaminase (GabT) in glutarate production via the new pathway responsible for nitrogen assimilation, which increased the glutarate titer to 7.7 ± 0.7 g/L, i.e., 40% higher than with two transaminases operating in glutarate biosynthesis. Flux enforcement was more effective with one coupling site, thus highlighting requirements regarding the modularity and stoichiometry of pathway-specific flux enforcement for microbial production.

Keywords: 5-aminovalerate; glutarate; bioplastics; polyamides; flux enforcement; *Corynebacterium glutamicum*

1. Introduction

Plastics are primarily synthesized chemically from petroleum and natural gas. However, the annual market volume of bioplastics is predicted to increase from 2.11 million tons in 2019 to 2.43 million tons in 2024 [1]. Among bioplastics, the biopolyamides find many applications ranging from the production of parachutes during World War II to filaments for 3D-printing at present [2,3]. Polyamides can be produced via two routes: either by the condensation of dicarboxylic acids with diamines or by the anionic ring-opening polymerization of lactams, which can be formed from ω -amino acids via cyclization [4]. Examples of these main building blocks range from succinate to sebacate for

dicarboxylic acids, from putrescine to hexamethylenediamine for diamines, and from γ -aminobutyrate (GABA) to ϵ -aminocaproate (6ACA) for ω -amino acids.

Monomeric polyamide precursors with a carbon chain length of 5 (C5) comprise the ω -amino acid 5-aminovalerate (5AVA) for ring-opening polymerization to polyamide 5 (PA 5), the diamine cadaverine, and the dicarboxylic acid glutarate for the co-polycondensation to PA 5.5 [5]. All three precursors can be synthesized from the amino acid L-lysine by a series of oxidation, decarboxylation, and deamination reactions; thus, fermentative routes for their production have been established. *Corynebacterium glutamicum* is well-known for the industrial production of L-lysine by fermentation, a process operated at about 2.6 million tons in 2018 [6]. L-lysine-overproducing *C. glutamicum* strains have been converted to cadaverine producers through the expression of a heterologous L-lysine decarboxylase gene (Figure 1A) [7], and high titers, yields, and productivities have been reached, e.g., using lignocellulose derived wastes [8,9].

For the production of 5AVA from L-lysine, two metabolic pathways have been developed. A three-step route to 5AVA that does not require molecular oxygen (Figure 1A) was established in our group, and it is compatible with aerobic fermentation that is typically limited by low oxygen transfer rates. This three-step LdcC–PatA–PatD route involves L-lysine decarboxylase, putrescine transaminase, and γ -aminobutyraldehyde dehydrogenase (encoded by the genes *ldcC*, *patA*, and *patD*, respectively) [10]. In shake flasks, 5AVA product titers of about 5 g/L, a yield of 0.13 g/g, and a volumetric productivity of 0.12 g/L/h were reached [10]. Independently, a two-step route based on *davAB*-encoded δ -aminovaleramidase and L-lysine monooxygenase from *Pseudomonas putida* has been used in *Escherichia coli* and *C. glutamicum* with product titers up to about 33 g/L [11–13]. The first reaction in the DavB–DavA route requires the presence of molecular oxygen for the oxidative decarboxylation prior to hydrolyzation from L-lysine via 5-aminovaleramide to 5AVA.

Glutarate can be derived from 5AVA by transamination and oxidation (Figure 1A). *C. glutamicum* possesses the *gabTD* operon encoding enzymes responsible for the catabolism and import of GABA, an ω -amino acid with a shorter chain length than 5AVA (C4 instead of C5). The *gabTD*-encoded GABA/5AVA aminotransferase, and succinate/glutarate semialdehyde dehydrogenase accept both C4 and C5 substrates [14]. These genes can be deleted to increase the production of 5AVA by preventing its degradation [10] or overexpressed to improve the conversion of 5AVA to glutarate [15]. Glutarate production via the five-step LdcC–PatA–PatD–GabT–GabD route (Figure 1A) was found to enable the fermentative production of glutarate up to 25 g/L [15]. Glutarate production has also been realized by employing the DavB–DavA–GabT–GabD route, and the produced glutarate was used with diaminoethane to prepare PA 6,6 [12,16].

The metabolic engineering strategy of flux enforcement couples a biosynthetic production pathway to a pathway required for growth [6]. The coupling of the production of 4-hydroxy-L-isoleucine via 2-oxoglutarate-dependent hydroxylase to growth by the deletion of the 2-oxoglutarate dehydrogenase subunit gene *sucA* was first described for *E. coli* [17]. In this application and in 4-hydroxy-L-proline production [18], the production pathways become part of an artificial TCA cycle. Flux enforcement by replacing a reaction of the TCA cycle was also used to improve L-lysine production by a succinyl-CoA synthetase-negative (Δ *sucCD*), L-lysine-producing *C. glutamicum* strain where the succinylase branch of L-lysine production metabolically complemented the disrupted TCA cycle [19].

Flux enforcement has also been applied to improve glutarate production by *C. glutamicum* [15]. The transamination reactions catalyzed by cadaverine/putrescine transaminase PatA and GABA/5AVA amino transferase GabT during glutarate production were coupled to growth in the absence of the major ammonium assimilating enzyme L-glutamic acid dehydrogenase Gdh [15] (Figure 1B). The resulting strain reached glutarate titers of about 5 g/L in shake flasks and about 25 g/L during fed-batch fermentation [15]. Here, the monooxygenase enzyme putrescine oxidase encoded by *pao* from *Rhodococcus qingshengii* or *Paenarthrobacter aureescens* was tested for the conversion of cadaverine to 5-aminopentanal in pathways for the production of 5AVA and glutarate (Figure 1A). We analyzed

whether flux enforcement by coupling *gdh* deletion to a single transaminase activity using this novel pathway was superior to its coupling to the two transaminases PatA and GabT for glutarate production.

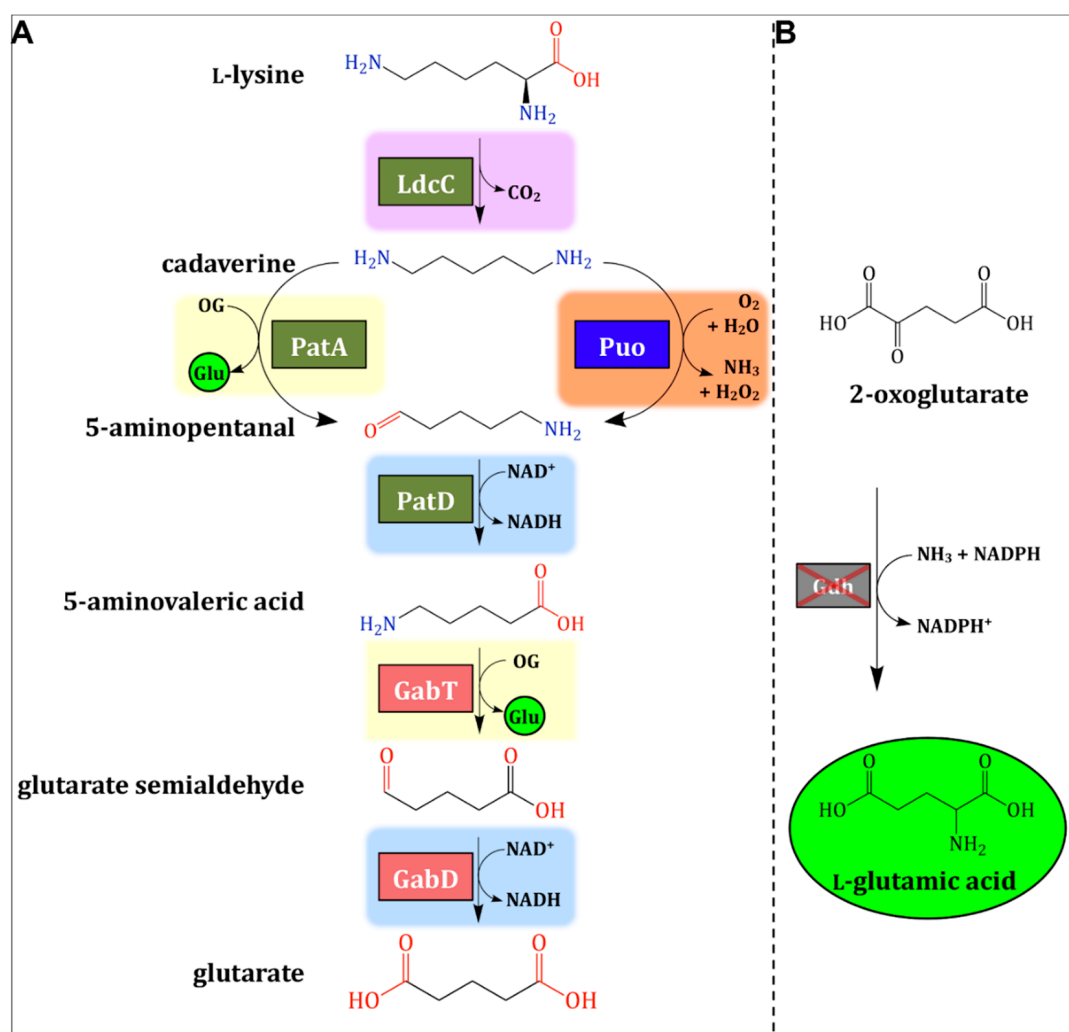


Figure 1. Fermentative production of 5-aminovalerate (5AVA) and glutarate. **(A)** A novel three-step metabolic pathway for production of 5AVA and glutarate was established by the exchange of a transaminase of an existing three-step pathway (PatA) with an oxidase (Puo). The anticipated shift of net nitrogen assimilation in the form of L-glutamic acid is counteracted by **(B)** endogenous L-glutamate synthesis by L-glutamic acid dehydrogenase (Gdh), which was deleted to enforce the flux towards glutarate. Pink areas depict decarboxylation reactions. Yellow areas depict transamination steps. Orange areas depict deamination steps. Blue areas depict oxidations. Red-shadowed genes (*gabT*, γ -aminobutyrate (GABA)/5AVA amino transferase; *gabD*, and succinate/glutarate-semialdehyde dehydrogenase) are native genes of *Corynebacterium glutamicum*. Additionally, copies of *gabTD* from *Pseudomonas stutzeri* were added by heterologous overexpression. The grey-shadowed gene (*gdh*, L-glutamic acid dehydrogenase) is native in *C. glutamicum*. The dark green-shadowed genes (*ldcC*, L-lysine decarboxylase; *patA*, putrescine transaminase; and *patD*, γ -aminobutyraldehyde dehydrogenase) are originally from *Escherichia coli* and were added by heterologous overexpression. The blue-shadowed gene (*puo*, putrescine oxidase; EC 1.4.3.10) was originally from *Rhodococcus qingshengii* and *Paenarthrobacter aureescens*, and it was heterologously expressed in *C. glutamicum*. L-glutamic acid is highlighted in bright green. OG: 2-oxoglutarate, Glu: L-glutamic acid.

2. Results

2.1. Design of the Study: Comparing Flux Enforcement with Either a Single or Two Coupling Sites

The five-step LdcC–PatA–PatD–GabT–GabD route from L-lysine to glutarate conserves the energy available to the cell in two ways. First, the oxidoreductases PatD and GabD yield the reduced redox cofactor NADH. Second, during the conversion of cadaverine to 5-aminopentanal and 5AVA to glutarate semialdehyde, the transaminases PatA and GabT simultaneously yield L-glutamic acid from the TCA cycle intermediate 2-oxoglutarate. The operation of the reactions of PatA and/or GabT in the glutarate production pathway obviates the need to synthesize L-glutamic acid from 2-oxoglutarate and ammonium by NADPH-dependent L-glutamic acid dehydrogenase, which is encoded by *gdh*. Indeed, flux enforcement by the deletion of *gdh* was found to improve glutarate production via the five-step LdcC–PatA–PatD–GabT–GabD route [15] because the deletion of *gdh* was compensated for by the activities of the two transaminases PatA and GabT. This prompted us to analyze whether flux enforcement by *gdh* deletion coupled to a single transaminase reaction in the glutarate pathway was superior to coupling to the two transaminases PatA and GabT.

The fourth reaction in the five-step reaction sequence (transamination by GabT) was kept in order to maintain the “metabolic pull” of flux enforcement by *gdh* deletion, while the second reaction (transamination by PatA) was chosen to be replaced by an oxidative deamination reaction. Unlike the 2-oxoglutarate-dependent transamination catalyzed by PatA, oxidative deamination by an oxidase does not yield L-glutamic acid; thus, it cannot bypass NADPH-dependent L-glutamic acid dehydrogenase. A search for oxidases that accept substrates similar to cadaverine was conducted. Indeed, putrescine oxidase (EC 1.4.3.10) encoded by *puo* from *Rhodococcus erythropolis* accepts cadaverine as a substrate with a catalytic efficiency (k_{cat}/K_m) of $220 \text{ s}^{-1} \text{ mM}^{-1}$ [20]. Another candidate from *Paenarthrobacter aurescens* also showed enzyme activity towards cadaverine, albeit with magnitudes lower k_{cat}/K_m ($4.78 \text{ s}^{-1} \text{ mM}^{-1}$) [21]. Both enzymes contain non-covalently bound FAD. The putrescine oxidase gene *puo_{Rq}* from *Rhodococcus qingshengii* was used due to the 98% identity similarity of its amino acid sequence to the characterized putrescine oxidase proteins from *R. erythropolis* [20] and the fact that genomic DNA from *R. qingshengii* was available from the strain collection Deutsche Sammlung von Mikroorganismen und Zellkulturen (DSMZ). The putrescine oxidases from *P. aurescens* (*puo_{Pa}*) and *R. qingshengii* (*puo_{Rq}*) were tested in the second position of the five-step pathway for conversion of L-lysine to glutarate in order to compare the new routes (LdcC–Puo_{Rq}–PatD–GabT–GabD and LdcC–Puo_{Pa}–PatD–GabT–GabD) to the reference route of LdcC–PatA–PatD–GabT–GabD.

2.2. Proof of Principle: Putrescine Oxidases Oxidatively Deaminate Cadaverine in *C. glutamicum*

To test whether the putrescine oxidases from *P. aurescens* and *R. qingshengii* catalyzed the oxidative deamination of cadaverine to 5AVA in *C. glutamicum*, 5AVA production via the three-step pathway was analyzed after replacing transamination by PatA with a putrescine oxidase. The putrescine oxidase genes from *P. aurescens* and *R. qingshengii*, respectively, were heterologously expressed in the L-lysine-producing *C. glutamicum* strain GSLA2 to generate the LdcC–Puo_{Rq}–PatD and LdcC–Puo_{Pa}–PatD variants of the reference three-step LdcC–PatA–PatD route. GSLA2 is based on GRLys1, which was obtained by genome reduction and rational metabolic engineering of L-lysine production [22–24], but it also lacks the genes *sugR*, *ldhA*, *snaA* and *cgmA* to improve glucose consumption and to avoid N-acetylation and the export of cadaverine [8,23,25–27]. The AVA1_{patA} reference strain produced $1.1 \pm 0.0 \text{ g/L}$ 5AVA in 3 mL microtiter plates (Figure 2A). Notably, the strains with the new LdcC–Puo_{Rq}–PatD and LdcC–Puo_{Pa}–PatD routes produced $0.4 \pm 0.0 \text{ g/L}$ 5AVA (AVA1_{puoRq}) and $0.1 \pm 0.0 \text{ g/L}$ 5AVA (AVA1_{puoPa}), respectively. Thus, a proof of concept for the fermentative production of 5AVA with putrescine oxidases was achieved.

The spectrum of by-products formed indicated the incomplete conversion of L-lysine to 5AVA since 1.1 ± 0.1 and 3.6 ± 0.3 g/L of L-lysine and 0.3 ± 0.0 and 0.1 ± 0.0 g/L of cadaverine accumulated in the cultivations with AVA1_puoRq and AVA1_puoPa, respectively (Figure 2A). This was not observed with the AVA1_patA reference strain. All strains produced glutarate (Figure 2A), which may be synthesized from 5AVA by endogenous, chromosomally encoded enzymes, namely GabT and GabD.

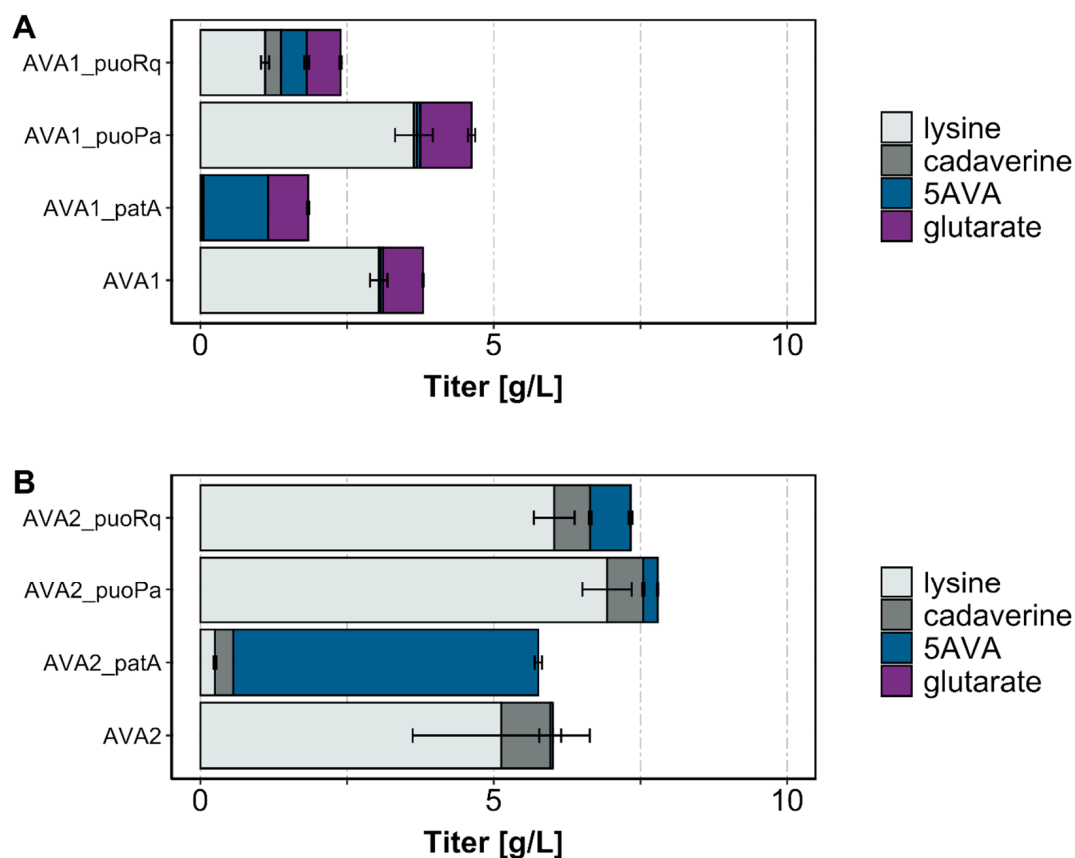


Figure 2. Production titers of 5AVA and by-products by strains derived from (A) *C. glutamicum* GSLA2(pVWEx1-*ldcC*) and (B) GSLA2Δ*gabTDP*(pVWEx1-*ldcC*). Three milliliter cultures were grown in the Duetz system with a 4% glucose minimal medium supplemented with 1 mM isopropyl β-d-1-thiogalactopyranoside (IPTG) and harvested after 48 h. Values and error bars represent mean and standard deviation values (n = 3 cultivations).

2.3. Deletion of Genes for Conversion of 5AVA to Glutarate and Change of the Microcultivation System Improved 5AVA Production

The accumulation of glutarate by the strains with the different three-step routes (LdcC–PatA–PatD, LdcC–PuoRq–PatD and LdcC–PuoPa–PatD) (Figure 2A) prompted us to delete the GABA utilization operon. The deletion of the *gabTDP* operon has previously been shown to abrogate glutarate formation when using the LdcC–PatA–PatD reference route [10]. The assumption was that this would abolish glutarate formation as a by-product of the new AVA2_puoRq and AVA2_puoPa strains. It was, in fact, shown to be correct because glutarate was not detected after 48 h of the 3 mL microtiter plate cultivation of AVA2_puoRq, AVA2_puoPa, and the reference strain AVA2_patA (Figure 2B). Compared to the strains possessing *gabTDP* operon (Figure 2A), the production of 5AVA increased two-to-five fold to final titers of 0.7 ± 0.0 g/L for AVA2_puoRq, 0.2 ± 0.0 g/L for AVA2_puoPa, and 5.2 ± 0.1 g/L for the reference strain AVA2_patA (Figure 2B). While the accumulation of cadaverine was comparable for the three strains, the *C. glutamicum* strains AVA2_puoRq and AVA2_puoPa accumulated L-lysine to

high concentrations (6.9 ± 0.4 and 6.0 ± 0.3 g/L, respectively; Figure 2B). This indicated the incomplete conversion of L-lysine to 5AVA by the AVA2_puoRq and AVA2_puoPa strains.

Since the putrescine oxidase reaction requires molecular oxygen, we analyzed 5AVA production in another microcultivation system while allowing for a higher oxygen transfer rate than the current system (i.e., a Duetz system with a cultivation volume of 3 mL at 220 rpm). We used a BioLector with different filling volumes (800, 1000, and 1200 μ L) at 1300 rpm, which are known to provide superior oxygen transfer rates [28,29]. Cultivation in the BioLector system lead to increased production of 5AVA by AVA2_puoRq about five-fold (3.5 ± 0.2 , 3.5 ± 0.5 , and 3.7 ± 0.4 g/L with filling volumes of 800, 1000, and 1200 μ L) in comparison to the Duetz system. 5AVA production by AVA2_puoPa was increased by about two-fold (0.4 ± 0.0 , 0.4 ± 0.0 , and 0.5 ± 0.1 g/L with filling volumes of 800, 1000, and 1200 μ L, respectively), as can be seen by comparing Figure 3 with Figure 2B. Notably, significantly less L-lysine was accumulated by the strain overexpressing puoRq than the strain overexpressing puoPa ($4.3\text{--}4.7$ g/L compared to 6.9 ± 0.4 g/L, respectively), as can be seen in Figure 3.

Taken together, cultivation with high oxygen transfer rates in the BioLector system improved 5AVA production by the new three step route and allowed us to identify the better performance of the LdcC-PuoRq-PatD variant than of the LdcC-PuoPa-PatD variant; however, the LdcC-PuoRq-PatD variant was found to be inferior to the LdcC-PatA-PatD route in regards to 5AVA production. Nevertheless, we continued to use the LdcC-PuoRq-PatD variant with the putrescine oxidase from *R. qingshengii* to test its performance for glutarate production and flux enforcement.

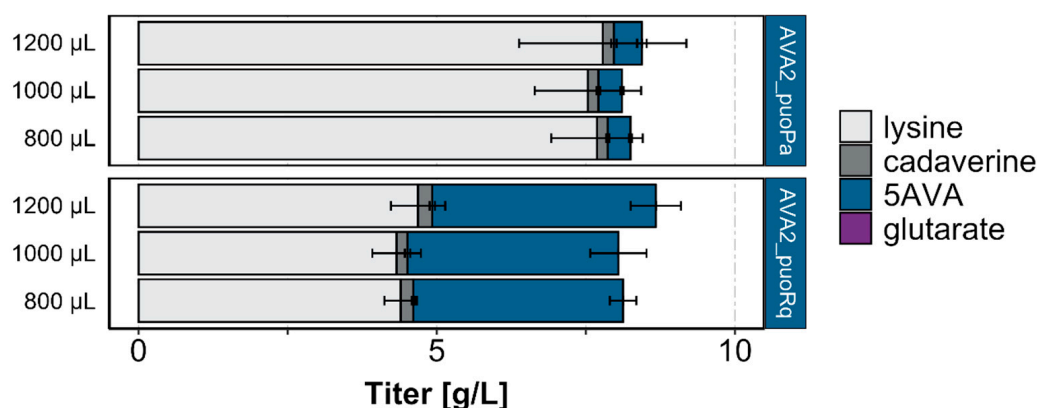


Figure 3. Production titers of 5AVA and by-products by strains derived from *C. glutamicum* GSLA2 Δ gabTDP (pVWEx1-ldcC). Cells were grown in a BioLector using different culture volumes (800–1200 μ L) of a 4% glucose minimal medium supplemented with 1 mM IPTG and harvested after 48 h. Values and error bars represent mean and standard deviation values ($n = 3$ cultivations).

2.4. Flux Enforcement by Deletion of the L-Glutamic Acid Dehydrogenase Gene Improved Glutarate Production

Production can be coupled to growth requirements by flux enforcement. The flux enforcement of glutarate production has been achieved by the deletion of the L-glutamic acid dehydrogenase gene in *C. glutamicum* [15]. L-glutamic acid dehydrogenase is the major reactant that is necessary for the assimilation of ammonium into L-glutamic acid in *C. glutamicum* [30]. 2-Oxoglutarate-dependent transaminase reactions in synthetic cascades can substitute for L-glutamic acid dehydrogenase if they operate in the direction of L-glutamic acid formation. In the five-step pathway from L-lysine to glutarate with LdcC, PatA, PatD, GabT, and GabD, L-glutamic acid is synthesized from 2-oxoglutarate by two reactions, namely those catalyzed by PatA and by GabT. Flux enforcement by the deletion of the L-glutamic acid dehydrogenase gene *gdh* has been shown to improve glutarate production [15].

We reasoned that the beneficial effect of *gdh* deletion for the flux enforcement of glutarate production may be more pronounced in a five-step pathway from L-lysine to glutarate that only involves a single transaminase reaction instead of two. Therefore, we constructed a strain that expressed the oxidase gene *puo_{Rq}* instead of the transaminase gene *patA*. The GSLA2G strain, which lacked *gdh* coding for L-glutamic acid dehydrogenase, was transformed with plasmids for the expression of either the LdcC–Puo_{Rq}–PatD–GabT–GabD variant with a single transaminase (GLUT_puoRq) or, as a reference, the LdcC–PatA–PatD–GabT–GabD variant with two transaminases (GLUT_patA). The GLUT_puoRq strain grew slower (0.08 ± 0.00 compared to 0.11 ± 0.00 1/h, respectively) and to an about 20% lower maximal biomass concentration (3.6 ± 0.1 compared to 4.5 ± 0.2 g/L cell dry weight, respectively) than the GLUT_patA reference strain. Importantly, while the by-product formation was similar for both strains, GLUT_puoRq produced about 40% more glutarate (7.7 ± 0.7 compared to 5.5 ± 0.2 g/L, respectively; Figure 4) than the reference strain GLUT_patA. This confirmed our hypothesis that flux enforcement by *gdh* deletion coupled to a production pathway with a single transaminase was superior to a route using two transaminase reactions as metabolic coupling sites.

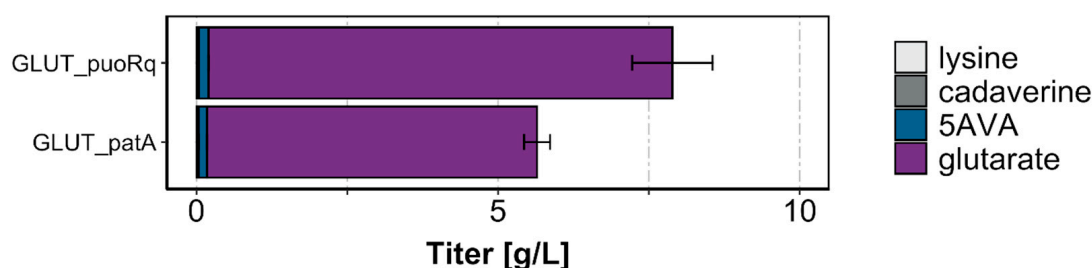


Figure 4. Production titers of glutarate and precursors by strains GLUT_puoRq and GLUT_patA. Cells were grown in the BioLector with a 4% glucose minimal medium supplemented with 1 mM IPTG and harvested after 72 h. Values and error bars represent mean and standard deviation values (n = 3 cultivations).

3. Discussion

This study showed that the oxidative deamination of cadaverine by putrescine oxidase Puo can operate in *C. glutamicum* to replace cadaverine transaminase PatA in synthetic pathways that convert cadaverine to 5AVA or glutarate. Studying glutarate biosynthesis pathways with either Puo or PatA allowed us to determine the effectiveness of flux enforcement (Figure 4). We showed how L-glutamic acid synthesis (which is required for growth) that is conducted by either one or two transamination reactions in the synthetic glutarate biosynthesis pathways can compensate for the absence of L-glutamic acid dehydrogenase caused by the deletion of its gene *gdh*. Glutarate production was higher when it was coupled to L-glutamic acid synthesis by one transamination (GabT) compared to a 1:2 stoichiometry, i.e., when L-glutamic acid was formed in reactions catalyzed by two transaminases (PatA and GabT) in the glutarate production pathway. Puo is not more efficient than PatA per se, because 5AVA production via the LdcC–PuoRq–PatD route was found to be lower than production via the LdcC–PatA–PatD route (Figure 2B). Thus, the better glutarate production via the LdcC–PuoRq–PatD–GabT–GabD route compared to the LdcC–PatA–PatD–GabT–GabD route (Figure 4) resulted from the better efficiency of flux enforcement with a single coupling site as compared to two coupling sites (Figure 1).

Putrescine oxidase belongs to the group of diamine oxidases found in bacteria, archaea and eukaryotes that are usually active with short aliphatic diamines in order to utilize them as carbon and/or nitrogen sources [31]. Applications in enzyme catalysis benefit from the fact that these flavoproteins utilize molecular oxygen as an electron acceptor instead of costly redox cofactors such as NAD(P)H [20,21,31,32], e.g., for the enzymatic transformation of cadaverine to 5-aminopentanal by a diamine oxidase [33]. One constraint to their application is the concomitant formation of hydrogen peroxide, an oxidative stressor that causes significant damage to the enzymes used in biocatalysis and to DNA and proteins in vivo [34]. As *C. glutamicum*, the production host chosen here, shows a high

natural resistance to hydrogen peroxide due to its very active catalase (commercialized as CAS Number 9001-05-2 [34]), pathways operating with putrescine oxidase functioned well. However, the decrease in the growth rate of the strains with Puo-supported glutarate production in comparison to strain with PatA-supported glutarate production may be attributed to H₂O₂ accumulation.

Aerobic fermentation processes are often limited by low oxygen transfer rates, which may be detrimental to growth and production, in particular for biosynthesis routes requiring molecular oxygen. Since putrescine oxidase requires molecular oxygen [31,35], cultivation platforms supporting different oxygen transfer rates (Duetz microtiter plates (MTPs) and BioLector MTPs) were compared [28,29]. Production was higher in the platform with the higher oxygen transfer rates (as can be seen by comparing Figures 2B and 3) in the strain where 5AVA production was based on oxidase activity. The observed benefit may not only have been due to the better provision of molecular oxygen for putrescine oxidase, since even when assessing only the production of precursor L-lysine, *C. glutamicum* requires a minimum oxygen transfer rate of 14 mmol L⁻¹ h⁻¹ for optimal biomass and L-lysine production, which cannot be reached in Duetz plates [29,36]. This oxygen bottleneck was also observed in closed tubes for an enzyme activity assay that employed the DavA–DavB route from L-lysine via 5-aminovaleramide to 5AVA, where *davB* encodes a L-lysine monooxygenase [12]. Thus, the better performance of the three-step LdcC–PatA–PatD pathway for the conversion of L-lysine to 5AVA compared to the variants with putrescine oxidase Puo_{Rq} or Puo_{Pa} instead of transaminase PatA (LdcC–Puo_{Rq}–PatD and LdcC–Puo_{Pa}–PatD) may also have been due the fact that transaminase PatA does not require molecular oxygen in oxygen-restricted conditions (Duetz MTPs).

The substrate spectrum of putrescine oxidase is relatively broad because, besides the C4 diamine putrescine and the C5 cadaverine, longer diamines (hexamethylenediamine, spermine, spermidine) are also accepted—though the shorter C3 diaminopropane is not [20]. This feature is not limited to the oxidases, as it is also true for the transaminases PatA and GabT (accepting substrates of different chain lengths: diamines such as putrescine and cadaverine and ω-amino acids such as GABA and 5AVA, respectively). Transaminases, in particular, are known for their promiscuity towards a broad range of substrates [37,38], which proves advantageous in the evolutionary sense but can translate to a drawback for short-term production experiments [39]. Nevertheless, the broad substrate spectra have been employed for the metabolic engineering of diamines, ω-amino acids, and dicarboxylic acids [14], though it has had to be ensured that only a precursor of one chain length was synthesized. This specificity has been achieved by narrow spectrum decarboxylases such as L-ornithine decarboxylase yielding putrescine from L-ornithine for the C4 products or, as also used here, L-lysine decarboxylase for C5 products [10,14,40].

The cascading of enzymes in biocatalysis [41] helps to overcome the need for the purification of intermediates, to regenerate redox cofactors [42], or to displace the reaction equilibrium towards product formation when coproducts tautomerize, dimerize, cyclize, or polymerize, as has been shown for self-sufficient transamination reactions [43]. Cascaded enzymes in metabolic pathways typically allow for coupling to cellular respiration, e.g., for redox cofactor regeneration in whole-cell biotransformations [44]. For fermentation processes, flux enforcement is a powerful tool to link production to an essential metabolic pathway. In *C. glutamicum*, L-lysine and glutarate production titers have benefitted from this technique [6,15,19]. Similarly, the metabolic cutoffs of genes in the pentose phosphate pathway have been found to enforce the co-utilization of pentoses with methanol by complementation with genes for methanol and formaldehyde assimilation [45,46].

Here, we compared flux enforcements with two or one coupling sites, specifically to see whether the synthesis of L-glutamic acid in the absence of L-glutamic acid dehydrogenase was enabled by GabT alone or by PatA and GabT if glutarate was produced. With one coupling site (GabT alone), the titer of glutarate was increased by 40% compared to two coupling sites (Figure 4). Theoretically, a change from a 2:1 stoichiometry to a 1:1 stoichiometry in flux enforcement should have increased the glutarate titer by 100%. Similar observations were published for the flux enforcement of L-lysine production by the deletion of the genes for the TCA cycle enzyme succinyl-CoA synthetase genes, and it was hypothesized

that bypassing reactions such as the glyoxylate shunt compensated, to some extent, for the lack of succinyl-CoA synthetase [19]. Similarly, bypassing reactions compensating for the lack of L-glutamic acid dehydrogenase may have reduced the beneficial effect of flux enforcement. In addition to L-glutamic acid dehydrogenase, *C. glutamicum* possesses the glutamine synthetase/glutamine-oxoglutarate amidotransferase (GS/GOGAT) system for L-glutamic acid synthesis and ammonium assimilation [47]. The combined reactions of glutamine synthetase and glutamine-oxoglutarate amidotransferase differ from L-glutamic acid dehydrogenase with the requirement for ATP; thus, the GS/GOGAT-encoding genes are only upon induced nitrogen starvation with basal expression at the nitrogen concentrations used here for growth and production [48,49]. Thus, it is conceivable that GS/GOGAT activity reduced the beneficial effect of flux enforcement by the *gdh* deletion observed here (Figure 4). The additional deletion of the GS/GOGAT genes in the *gdh* deletion strain is not helpful because L-glutamic acid dehydrogenase and the GS/GOGAT system are the only pathways for net ammonium assimilation, whereas transaminases only transfer ammonium from an existing donor to an oxoacid acceptor.

Glutarate production may be rationally improved through metabolic engineering targeting, e.g., precursor supply, redox cofactor regeneration, or by-product formation [50], as well as by enzyme engineering, e.g., targeting catalytic efficiency or the product inhibition of the synthetic glutarate biosynthesis pathway [51]. Recently, the application of adaptive laboratory evolution (ALE), which has revealed answers to fundamental evolutionary questions in *E. coli* [52,53], gained attention in strain development for growth-associated fermentative processes [54]. In *C. glutamicum*, ALE has been exploited for increased methanol-dependent growth and tolerance, followed by whole-genome sequencing and mutational analysis, respectively [45,55,56]. Notably, flux enforcement by *gdh* deletion in the glutarate-producing strains described here and previously [15] reduced the growth rate. Thus, it may be possible to accelerate glutarate production by this strain through ALE and to rationalize the selected genomic changes by reverse genetics. Importantly, reaching the industrial maturity of glutarate production by recombinant *C. glutamicum* genetic and metabolic robustness, as well the scaling-up of such production, remains to be achieved.

4. Materials and Methods

4.1. Microorganisms and Cultivation Conditions

The *E. coli* DH5 α strain was used as a cloning host [57], grown in lysogeny broth (LB) at 37 °C, and supplemented with antibiotics (50 $\mu\text{g mL}^{-1}$ kanamycin, 100 $\mu\text{g mL}^{-1}$ spectinomycin, and 10 $\mu\text{g mL}^{-1}$ tetracycline) when appropriate. *C. glutamicum* ATCC13032-derived strains were cultivated in brain heart infusion with 0.5 M sorbitol (BHIS) or an Eggeling and Bott 2005 CGXII minimal medium supplemented with 25 $\mu\text{g mL}^{-1}$ kanamycin, 100 $\mu\text{g mL}^{-1}$ spectinomycin, 5 $\mu\text{g mL}^{-1}$ tetracycline, and 1 mM IPTG when appropriate. All bacterial strains and plasmids are listed in Tables 1 and 2. For growth experiments with *C. glutamicum*, overnight cultures in 50 mL of BHIS were harvested and washed twice in a CGXII medium before inoculation to an OD₆₀₀ of 1 and supplementation with 4% (*w/v*) glucose as a sole carbon source. Growth in 10 mL Duetz MTPs with culture volumes of 3 mL at 220 rpm in an Ecotron ET25-TA-RC (Infors HT, Einsbach, Germany) was monitored for the determination of the OD₆₀₀ with a V-1200 Spectrophotometer (VWR, Radnor, PA, USA). The cultivations in the BioLector micro fermentation system (m2p-labs, Baesweiler, Germany) were performed in 3.2 mL FlowerPlates at 1300 rpm with filling volumes of 800, 1000, and 1200 μL .

Table 1. Bacterial strains used in this study.

Strain	Relevant Characteristics	Reference
<i>E. coli</i> DH5 α	$\Delta lacU169$ ($\phi 80lacZ$ $\Delta M15$), <i>supE44</i> , <i>hsdR17</i> , <i>recA1</i> , <i>endA1</i> , <i>gyrA96</i> , <i>thi-1</i> , <i>relA1</i>	[54]
<i>C. glutamicum</i> GRLys1 (DM1933 Δ CGP123)	<i>C. glutamicum</i> ATCC13032 with modifications: Δpck , <i>pyc</i> ^{P458S} , <i>hom</i> ^{V59A} , 2 copies of <i>lysC</i> ^{T3111} , 2 copies of <i>asd</i> , 2 copies of <i>dapA</i> , 2 copies of <i>dapB</i> , 2 copies of <i>ddh</i> , 2 copies of <i>lysA</i> , 2 copies of <i>lysE</i> , in-frame deletion of prophages CGP1 (cg1507-cg1524), CGP2 (cg1746-cg1752) and CGP3 (cg1890-cg2071).	[55]
GSLA2	GRLys1 with in-frame deletions: <i>sugR</i> (cg2115), <i>ldhA</i> (cg3219), <i>snaA</i> (cg1722), <i>cgmA</i> (cg2893)	[15]
GSLA2 Δ <i>gabTDP</i>	GSLA2 with in-frame deletions: <i>gabT</i> , <i>gabD</i> and <i>gabP</i> (cg0566-cg0568)	[10]
GSLA2G	GSLA2 with in-frame deletion: <i>gdh</i> (cg2280)	[15]
AVA1	GSLA2(pVWEx1- <i>ldcC</i>)(pEC-XT99A)	[10]
AVA1- <i>patA</i>	GSLA2(pVWEx1- <i>ldcC</i>)(pEKEEx3- <i>patDA</i>)	[10]
AVA1- <i>puoPa</i>	GSLA2(pVWEx1- <i>ldcC</i>)(pEC-XT99A- <i>puoPa-patD</i>)	This study
AVA1- <i>puoRq</i>	GSLA2(pVWEx1- <i>ldcC</i>)(pEC-XT99A- <i>puoRq-patD</i>)	This study
AVA2	GSLA2 Δ <i>gabTDP</i> (pVWEx1- <i>ldcC</i>)(pEC-XT99A)	[15]
AVA2- <i>patA</i>	GSLA2 Δ <i>gabTDP</i> (pVWEx1- <i>ldcC</i>)(pEKEEx3- <i>patDA</i>)	[15]
AVA2- <i>puoPa</i>	GSLA2 Δ <i>gabTDP</i> (pVWEx1- <i>ldcC</i>)(pEC-XT99A- <i>puoPa-patD</i>)	This study
AVA2- <i>puoRq</i>	GSLA2 Δ <i>gabTDP</i> (pVWEx1- <i>ldcC</i>)(pEC-XT99A- <i>puoRq-patD</i>)	This study
GLUT- <i>patA</i>	GSLA2G(pVWEx1- <i>ldcC</i>)(pEKEEx3- <i>patDA</i>)(pEC-XT99A- <i>gabTD</i> ^{Pstu})	[15]
GLUT- <i>puoRq</i>	GSLA2G(pVWEx1- <i>ldcC</i>)(pEKEEx3- <i>puoRq-patD</i>)(pEC-XT99A- <i>gabTD</i> ^{Pstu})	This study

Table 2. Plasmids used in this study.

Plasmid	Relevant Characteristics	Reference
pBV2xp	Amp ^R , Kan ^R , <i>B. methanolicus</i> / <i>E. coli</i> shuttle vector, pHCMC04 derivative, P _{xy1} from <i>B. megaterium</i>	[56]
pBV2xp- <i>puoRq-patD</i>	pBV2xp-expressing <i>puo</i> from <i>R. qingshengii</i> and <i>patD</i> from <i>E. coli</i> MG1655	This study
pBV2xp- <i>puoPa-patD</i>	pBV2xp-expressing <i>puo</i> from <i>P. aurescens</i> and <i>patD</i> from <i>E. coli</i> MG1655	This study
pEC-XT99A	Tet ^R , <i>C. glutamicum</i> / <i>E. coli</i> shuttle vector (P _{trc} , <i>lacI</i> ^q , pGA1 <i>oriV</i> _{Cg})	[57]
pEC-XT99A- <i>gabTD</i> ^{Pstu}	pEC-XT99A-expressing <i>gabT</i> and <i>gabD</i> from <i>Pseudomonas stutzerii</i> ATCC17588	[15]
pEC-XT99A- <i>puoPa-patD</i>	pEC-XT99A-expressing <i>puo</i> from <i>P. aurescens</i> and <i>patD</i> from <i>E. coli</i> MG1655	This study
pEC-XT99A- <i>puoRq-patD</i>	pEC-XT99A-expressing <i>puo</i> from <i>R. qingshengii</i> and <i>patD</i> from <i>E. coli</i> MG1655	This study
pEKEEx3	Spec ^R , <i>C. glutamicum</i> / <i>E. coli</i> shuttle vector (P _{tac} <i>lacI</i> ^q pBL1, <i>oriV</i> _{Ec})	[58]
pEKEEx3- <i>patDA</i>	pEKEEx3-expressing <i>patD</i> and <i>patA</i> from <i>E. coli</i> MG1655	[15]
pEKEEx3- <i>puoRq-patD</i>	pEKEEx3-expressing <i>puo</i> from <i>R. qingshengii</i> and <i>patD</i> from <i>E. coli</i> MG1655	This study
pVWEx1- <i>ldcC</i>	pVWEx1-expressing <i>ldcC</i> from <i>E. coli</i> MG1655	[38]

4.2. Molecular Biology Methods

The isolation of the genomic DNA of *C. glutamicum* and classical methods that include the plasmid isolation, molecular cloning, and heat-shock transformation of *E. coli* and the electroporation of *C. glutamicum* were performed as described previously [58,59]. ALLin HiFi DNA Polymerase (HighQu, Kraichtal, Germany) was used to amplify DNA sequences, with plasmid or genomic DNA used as the template. The oligonucleotides that were used as primers in this study are listed in Table 3.

The genomic DNA (gDNA) of *Rhodococcus qingshengii* (DSM 45257) and *Paenarthrobacter aurescens* (DSM 20116) was obtained from the German Collection of Microorganisms and Cell Cultures (DSMZ), and the gDNA of *E. coli* MG1655 was isolated in [58]. The pBV2xp plasmid was digested with the

restriction enzymes BamHI and SacI (New England Biolabs, Ipswich, MA, USA). The DNA fragments were joined by the means of isothermal DNA assembly [60].

Table 3. Oligonucleotides used as primers in this study.

Primer	Sequence (5'–3')	Description
AVA25	ttcacttaaggggaaatggcaaatgcagaatctgatcgcgactgtgatcgtcgg	Putrescine oxidase gene from <i>P. aurescens</i> 579_fw
AVA30	tcttactacctctatttatgtaattgttactcaggcgacaggtacagaagccaactgtt	Putrescine oxidase gene from <i>P. aurescens</i> 579_rv
AVA27	ttcacttaaggggaaatggcaaatgcctactctccagagagacgttgcaatcgt	Putrescine oxidase gene from <i>R. qingshengii</i> djl-6-2_fw
AVA31	tcttactacctctatttatgtaattgttactcaggcctgtcgcgagcgtgatgt	Putrescine oxidase gene from <i>R. qingshengii</i> djl-6-2_rv
AVA32	gtaacaattacataaataaggaggtagtaagaatgcaacataagtactgattaacgg agaactggtag	γ -aminobutyraldehyde dehydrogenase gene from <i>E. coli</i> MG1655_fw
AVA33	acgacggccagtgaattcagctttaatgtttaacctgacgtggcggacga	γ -aminobutyraldehyde dehydrogenase gene from <i>E. coli</i> MG1655_rv
AVA43	agctggacacctctctctc	Sequencing of pBV2xp- <i>puo</i> _{Pa} - <i>patD</i>
AVA44	gcgcttacgttccagctac	Sequencing of pBV2xp- <i>puo</i> _{Pa} - <i>patD</i>
AVA45	ggcaggcgtgattaacatac	Sequencing of pBV2xp- <i>puo</i> _{Pa} - <i>patD</i> and pBV2xp- <i>puo</i> _{Rq} - <i>patD</i>
AVA48	cgcatctcgacacagtctc	Sequencing of pBV2xp- <i>puo</i> _{Rq} - <i>patD</i>
AVA49	caccgctacggcgggattc	Sequencing of pBV2xp- <i>puo</i> _{Rq} - <i>patD</i>
PXPF	tgttatccaccgaactaag	Colony PCR primer for pBV2xp_fw
BVXR	ccgcacagatgcgtaaggag	Colony PCR primer for pBV2xp_rv
patD_F	ccctgcgggaaattagaagaaaaggagggtttttatgcaacataagtactgatt aacggagaactgg	Construction of pEC-XT99A/pEKEx3- <i>puo</i> _{Rq} - <i>patD</i> _fw
patD_R	cctgcaggctgactctagatgtaattgtttaacctgacgtggcgg	Construction of pEC-XT99A/pEKEx3- <i>puo</i> _{Rq} - <i>patD</i> _rv
puoRq_F	attcagctcggtagaccgggcatattcacaaccttaattataaaggaggt ctttatgctactctccagagagacg	Construction of pEC-XT99A- <i>puo</i> _{Rq} - <i>patD</i> _fw
puoRq_R	cttctaatttcccacagggcaggtcctgtcgcgagc	Construction of pEC-XT99A- <i>puo</i> _{Rq} - <i>patD</i> _rv
puoPa_F	attcagctcggtagaccgggcccggtaacggccaacagtag aaaggaggtattttatgcagaatcttgatcgcgacg	Construction of pEC-XT99A- <i>puo</i> _{Pa} - <i>patD</i> _fw
puoPa_R	cttctaatttcccacagggcaggtcaggtacagaaagcc	Construction of pEC-XT99A- <i>puo</i> _{Pa} - <i>patD</i> _rv
puoRq_F2	cctgcaggctgactctagagccatattcacaaccttaattataaaggaggtctttt atgctactctccagagagacg	Construction of pEKEx3- <i>puo</i> _{Rq} - <i>patD</i> _fw
patD_R2	attcagctcggtagaccgggtaattgtttaacctgacgtggcgg	Construction of pEKEx3- <i>puo</i> _{Rq} - <i>patD</i> _rv
pEC_F	gcccgcacataacagg	Colony PCR primer for pEC-XT99A_fw
pEC_R	ggcgtttcactctgagttcgg	Colony PCR primer for pEC-XT99A_rv
pEK_F	cgcttccacttttcccgcgt	Colony PCR primer for pEKEx3_fw
pEK_R	gcatttatcagggtattgtc	Colony PCR primer for pEKEx3_rv
seq_patD	atcgaccgtggaattatccgc	Sequencing of pEC-XT99A/pEKEx3- <i>puo</i> _{Rq} - <i>patD</i>
seq1_Rq	gcgatctcgacacagtctcc	Sequencing of pEC-XT99A/pEKEx3- <i>puo</i> _{Rq} - <i>patD</i>
seq2_Rq	caacaccaaccacgaggacg	Sequencing of pEC-XT99A/pEKEx3- <i>puo</i> _{Rq} - <i>patD</i>
seq1_Pa	tggacacctctcttccacc	Sequencing of pEC-XT99A- <i>puo</i> _{Pa} - <i>patD</i>
seq2_Pa	acaccaaccacggagattcc	Sequencing of pEC-XT99A- <i>puo</i> _{Pa} - <i>patD</i>

To overexpress *puo*_{Rq}, *puo*_{Pa}, and *patD* in *C. glutamicum*, their genes were amplified from pBV2xp-*puo*_{Rq}-*patD*, pBV2xp-*puo*_{Pa}-*patD*, and the genomic DNA of *C. glutamicum*, respectively, and they were assembled into BamHI-linearized pEKEx3 and pEC-XT99A by Gibson Assembly using the respective primers. *C. glutamicum* was transformed with the constructed plasmids and empty vectors.

4.3. HPLC Analysis

The quantification of amino acids and cadaverine and glutarate in the cultivation medium was performed with a high-pressure liquid chromatography system (1200 series, Agilent Technologies Deutschland GmbH, Böblingen, Germany), as described previously [61]. After the centrifugation of 1 mL cell cultures at 14000 rpm for 10 min, the supernatant was stored at -20°C prior to analysis.

The amino acids L-lysine and 5AVA and the diamine cadaverine were detected with a fluorescence detector (FLD G1321A, 1200 series, Agilent Technologies) after the derivatization of the samples with OPA (ortho-phthalaldehyde). The detection of glutarate was done with a refractive index detector (RID G1362A, 1200 series, Agilent Technologies) and a diode array detector (DAD G1315B, 1200 series, Agilent Technologies).

5. Conclusions

By exchanging a putrescine transaminase with an oxidase in a synthetic glutarate pathway in *C. glutamicum*, a proof of concept for the production of 5AVA and glutarate was achieved. The heterologous expression of putrescine oxidase from two strains, *R. qingshengii* and *P. aurescens*, showed 5AVA production titers of 0.4 ± 0.0 and 0.1 ± 0.0 g/L 5AVA, respectively, and could be improved by the deletion of the glutarate module *gabTDP* and improved oxygen availability to a maximum of 3.7 ± 0.4 g/L 5AVA with the LdcC–PuOR_q–PatA–GabT–GabD route. Upon the disruption of *gdh*, which encodes the enzyme that is responsible for the major nitrogen assimilation reaction in *C. glutamicum*, the focus of the flux enforcement towards glutarate production tightened on a single transaminase reaction, as compared to the two transaminases PatA and GabT, resulting in a product titer increase of 40% (7.7 ± 0.7 vs. 5.5 ± 0.2 g/L). These results highlight requirements regarding the modularity and stoichiometry of the pathway-specific flux enforcement for microbial production.

Author Contributions: C.H. and V.F.W. conceptualized this work. B.D. investigated the underlying pathways. C.H. and M.I. constructed strains. C.H. performed the experiments. C.H. and V.F.W. analyzed the data. C.H. drafted, all authors revised, and V.F.W. finalized the manuscript. V.F.W. and S.H. supervised this work. All authors have read and agreed to the final version of the manuscript.

Funding: This work was funded by the ERA CoBioTech project C1Pro (FNR-22023617; ANR-17-COBI-0003-05).

Acknowledgments: The authors thank Carina Prell and Helena Schulz-Mirbach for technical support.

Conflicts of Interest: The authors declare no conflict of interest.

References

1. Bioplastics Market. Available online: <https://www.european-bioplastics.org/market/> (accessed on 15 September 2020).
2. Ali, M.A.; Kaneko, T. Polyamide Syntheses. In *Encyclopedia of Polymeric Nanomaterials*; Kobayashi, S., Müllen, K., Eds.; Springer: Berlin/Heidelberg, Germany, 2015; pp. 1750–1762. ISBN 978-3-642-29647-5.
3. Ligon, S.C.; Liska, R.; Stampfl, J.; Gurr, M.; Mülhaupt, R. Polymers for 3D Printing and Customized Additive Manufacturing. *Chem. Rev.* **2017**, *117*, 10212–10290. [[CrossRef](#)] [[PubMed](#)]
4. Radzik, P.; Leszczyńska, A.; Pielichowski, K. Modern biopolyamide-based materials: Synthesis and modification. *Polym. Bull.* **2020**, *77*, 501–528. [[CrossRef](#)]
5. Adkins, J.; Jordan, J.; Nielsen, D.R. Engineering *Escherichia coli* for renewable production of the 5-carbon polyamide building-blocks 5-aminovalerate and glutarate. *Biotechnol. Bioeng.* **2013**, *110*, 1726–1734. [[CrossRef](#)] [[PubMed](#)]
6. Wendisch, V.F. Metabolic engineering advances and prospects for amino acid production. *Metab. Eng.* **2020**, *58*, 17–34. [[CrossRef](#)]
7. Mimitsuka, T.; Sawai, H.; Hatsu, M.; Yamada, K. Metabolic Engineering of *Corynebacterium glutamicum* for Cadaverine Fermentation. *Biosci. Biotechnol. Biochem.* **2007**, *71*, 2130–2135. [[CrossRef](#)]
8. Kind, S.; Kreye, S.; Wittmann, C. Metabolic engineering of cellular transport for overproduction of the platform chemical 1,5-diaminopentane in *Corynebacterium glutamicum*. *Metab. Eng.* **2011**, *13*, 617–627. [[CrossRef](#)]
9. Wendisch, V.F.; Mindt, M.; Pérez-García, F. Biotechnological production of mono- and diamines using bacteria: Recent progress, applications, and perspectives. *Appl. Microbiol. Biotechnol.* **2018**, *102*, 3583–3594. [[CrossRef](#)]
10. Jorge, J.M.P.; Pérez-García, F.; Wendisch, V.F. A new metabolic route for the fermentative production of 5-aminovalerate from glucose and alternative carbon sources. *Bioresour. Technol.* **2017**. [[CrossRef](#)]

11. Fothergill, J.C.; Guest, J.R. Catabolism of L-Lysine by *Pseudomonas aeruginosa*. *J. Gen. Microbiol.* **1977**, *99*, 139–155. [[CrossRef](#)]
12. Rohles, C.M.; Gießelmann, G.; Kohlstedt, M.; Wittmann, C.; Becker, J. Systems metabolic engineering of *Corynebacterium glutamicum* for the production of the carbon-5 platform chemicals 5-aminovalerate and glutarate. *Microb. Cell Factories* **2016**, *15*. [[CrossRef](#)]
13. Shin, J.H.; Park, S.H.; Oh, Y.H.; Choi, J.W.; Lee, M.H.; Cho, J.S.; Jeong, K.J.; Joo, J.C.; Yu, J.; Park, S.J.; et al. Metabolic engineering of *Corynebacterium glutamicum* for enhanced production of 5-aminovaleric acid. *Microb. Cell Factories* **2016**, *15*. [[CrossRef](#)] [[PubMed](#)]
14. Chae, T.U.; Ahn, J.H.; Ko, Y.-S.; Kim, J.W.; Lee, J.A.; Lee, E.H.; Lee, S.Y. Metabolic engineering for the production of dicarboxylic acids and diamines. *Metab. Eng.* **2020**, *58*, 2–16. [[CrossRef](#)] [[PubMed](#)]
15. Pérez-García, F.; Jorge, J.M.P.; Dreyszas, A.; Risse, J.M.; Wendisch, V.F. Efficient Production of the Dicarboxylic Acid Glutarate by *Corynebacterium glutamicum* via a Novel Synthetic Pathway. *Front. Microbiol.* **2018**, *9*, 2589. [[CrossRef](#)] [[PubMed](#)]
16. Rohles, C.M.; Gläser, L.; Kohlstedt, M.; Gießelmann, G.; Pearson, S.; del Campo, A.; Becker, J.; Wittmann, C. A bio-based route to the carbon-5 chemical glutaric acid and to bionylon-6,5 using metabolically engineered *Corynebacterium glutamicum*. *Green Chem.* **2018**, *20*, 4662–4674. [[CrossRef](#)]
17. Smirnov, S.V.; Kodera, T.; Samsonova, N.N.; Kotlyarova, V.A.; Rushkevich, N.Y.; Kivero, A.D.; Sokolov, P.M.; Hibi, M.; Ogawa, J.; Shimizu, S. Metabolic engineering of *Escherichia coli* to produce (2S, 3R, 4S)-4-hydroxyisoleucine. *Appl. Microbiol. Biotechnol.* **2010**, *88*, 719–726. [[CrossRef](#)]
18. Theodosiou, E.; Breisch, M.; Julsing, M.K.; Falcioni, F.; Bühler, B.; Schmid, A. An artificial TCA cycle selects for efficient α -ketoglutarate dependent hydroxylase catalysis in engineered *Escherichia coli*: Strain Design for Proline Hydroxylation in Vivo. *Biotechnol. Bioeng.* **2017**, *114*, 1511–1520. [[CrossRef](#)]
19. Kind, S.; Becker, J.; Wittmann, C. Increased lysine production by flux coupling of the tricarboxylic acid cycle and the lysine biosynthetic pathway—Metabolic engineering of the availability of succinyl-CoA in *Corynebacterium glutamicum*. *Metab. Eng.* **2013**, *15*, 184–195. [[CrossRef](#)]
20. van Hellemond, E.W.; van Dijk, M.; Heuts, D.P.H.M.; Janssen, D.B.; Fraaije, M.W. Discovery and characterization of a putrescine oxidase from *Rhodococcus erythropolis* NCIMB 11540. *Appl. Microbiol. Biotechnol.* **2008**, *78*, 455–463. [[CrossRef](#)]
21. Lee, J.-I.; Jang, J.-H.; Yu, M.-J.; Kim, Y.-W. Construction of a Bifunctional Enzyme Fusion for the Combined Determination of Biogenic Amines in Foods. *J. Agric. Food Chem.* **2013**, *61*, 9118–9124. [[CrossRef](#)]
22. Baumgart, M.; Unthan, S.; Rückert, C.; Sivalingam, J.; Grünberger, A.; Kalinowski, J.; Bott, M.; Noack, S.; Frunzke, J. Construction of a Prophage-Free Variant of *Corynebacterium glutamicum* ATCC 13032 for Use as a Platform Strain for Basic Research and Industrial Biotechnology. *Appl. Environ. Microbiol.* **2013**, *79*, 6006–6015. [[CrossRef](#)]
23. Pérez-García, F.; Peters-Wendisch, P.; Wendisch, V.F. Engineering *Corynebacterium glutamicum* for fast production of L-lysine and L-pipecolic acid. *Appl. Microbiol. Biotechnol.* **2016**, *100*, 8075–8090. [[CrossRef](#)] [[PubMed](#)]
24. Unthan, S.; Baumgart, M.; Radek, A.; Herbst, M.; Siebert, D.; Brühl, N.; Bartsch, A.; Bott, M.; Wiechert, W.; Marin, K.; et al. Chassis organism from *Corynebacterium glutamicum*—A top-down approach to identify and delete irrelevant gene clusters. *Biotechnol. J.* **2015**, *10*, 290–301. [[CrossRef](#)] [[PubMed](#)]
25. Engels, V.; Lindner, S.N.; Wendisch, V.F. The global repressor SugR controls expression of genes of glycolysis and of the L-lactate dehydrogenase LdhA in *Corynebacterium glutamicum*. *J. Bacteriol.* **2008**, *190*, 8033–8044. [[CrossRef](#)] [[PubMed](#)]
26. Nguyen, A.Q.D.; Schneider, J.; Wendisch, V.F. Elimination of polyamine N-acetylation and regulatory engineering improved putrescine production by *Corynebacterium glutamicum*. *J. Biotechnol.* **2015**, *201*, 75–85. [[CrossRef](#)] [[PubMed](#)]
27. Lubitz, D.; Jorge, J.M.P.; Pérez-García, F.; Taniguchi, H.; Wendisch, V.F. Roles of export genes *cgmA* and *lysE* for the production of L-arginine and L-citrulline by *Corynebacterium glutamicum*. *Appl. Microbiol. Biotechnol.* **2016**, *100*, 8465–8474. [[CrossRef](#)]
28. Funke, M.; Diederichs, S.; Kensy, F.; Müller, C.; Büchs, J. The Baffled Microtiter Plate: Increased Oxygen Transfer and Improved Online Monitoring in Small Scale Fermentations. *Biotechnol. Bioeng.* **2009**, *103*, 1118–1128. [[CrossRef](#)]

29. Duetz, W.A.; Rüedi, L.; Hermann, R.; O'Connor, K.; Büchs, J.; Witholt, B. Methods for Intense Aeration, Growth, Storage, and Replication of Bacterial Strains in Microtiter Plates. *Appl. Environ. Microbiol.* **2000**, *66*, 2641–2646. [[CrossRef](#)]
30. Tesch, M.; de Graaf, A.A.; Sahm, H. In Vivo Fluxes in the Ammonium-Assimilatory Pathways in *Corynebacterium glutamicum* Studied by ¹⁵N Nuclear Magnetic Resonance. *Appl. Environ. Microbiol.* **1999**, *65*, 1099–1109. [[CrossRef](#)]
31. Floris, G.; Finazzi Agrò, A. Amine Oxidases. In *Encyclopedia of Biological Chemistry*; Elsevier: Amsterdam, The Netherlands, 2013; pp. 87–90. ISBN 978-0-12-378631-9.
32. Lee, J.-I.; Kim, Y.-W. Characterization of amine oxidases from *Arthrobacter aurescens* and application for determination of biogenic amines. *World J. Microbiol. Biotechnol.* **2013**, *29*, 673–682. [[CrossRef](#)]
33. Nau, W.M.; Ghale, G.; Hennig, A.; Bakirci, H.; Bailey, D.M. Substrate-Selective Supramolecular Tandem Assays: Monitoring Enzyme Inhibition of Arginase and Diamine Oxidase by Fluorescent Dye Displacement from Calixarene and Cucurbituril Macrocycles. *J. Am. Chem. Soc.* **2009**, *131*, 11558–11570. [[CrossRef](#)]
34. Milse, J.; Petri, K.; Rückert, C.; Kalinowski, J. Transcriptional response of *Corynebacterium glutamicum* ATCC 13032 to hydrogen peroxide stress and characterization of the OxyR regulon. *J. Biotechnol.* **2014**, *190*, 40–54. [[CrossRef](#)]
35. Romero, E.; Gómez Castellanos, J.R.; Gadda, G.; Fraaije, M.W.; Mattevi, A. Same Substrate, Many Reactions: Oxygen Activation in Flavoenzymes. *Chem. Rev.* **2018**, *118*, 1742–1769. [[CrossRef](#)] [[PubMed](#)]
36. Käß, F.; Prasad, A.; Tillack, J.; Moch, M.; Giese, H.; Büchs, J.; Wiechert, W.; Oldiges, M. Rapid assessment of oxygen transfer impact for *Corynebacterium glutamicum*. *Bioprocess Biosyst. Eng.* **2014**, *37*, 2567–2577. [[CrossRef](#)] [[PubMed](#)]
37. Jensen, R.A. Enzyme Recruitment in Evolution of New Function. *Annu. Rev. Microbiol.* **1976**, *30*, 409–425. [[CrossRef](#)]
38. Wilding, M.; Peat, T.S.; Kalyaanamoorthy, S.; Newman, J.; Scott, C.; Jermiin, L.S. Reverse engineering: Transaminase biocatalyst development using ancestral sequence reconstruction. *Green Chem.* **2017**, *19*, 5375–5380. [[CrossRef](#)]
39. Atkins, W.M. Biological messiness vs. biological genius: Mechanistic aspects and roles of protein promiscuity. *J. Steroid Biochem. Mol. Biol.* **2015**, *151*, 3–11. [[CrossRef](#)]
40. Jorge, J.M.P.; Leggewie, C.; Wendisch, V.F. A new metabolic route for the production of gamma-aminobutyric acid by *Corynebacterium glutamicum* from glucose. *Amino Acids* **2016**, *48*, 2519–2531. [[CrossRef](#)]
41. Gröger, H. Biocatalytic concepts for synthesizing amine bulk chemicals: Recent approaches towards linear and cyclic aliphatic primary amines and ω -substituted derivatives thereof. *Appl. Microbiol. Biotechnol.* **2019**, *103*, 83–95. [[CrossRef](#)]
42. Breuer, M.; Ditrich, K.; Habicher, T.; Hauer, B.; Keßeler, M.; Stürmer, R.; Zelinski, T. Industrial Methods for the Production of Optically Active Intermediates. *Angew. Chem. Int. Ed.* **2004**, *43*, 788–824. [[CrossRef](#)]
43. Grigoriou, S.; Kugler, P.; Kulcinskaja, E.; Walter, F.; King, J.; Hill, P.; Wendisch, V.F.; O'Reilly, E. Development of a *Corynebacterium glutamicum* bio-factory for self-sufficient transaminase reactions. *Green Chem.* **2020**, *22*, 4128–4132. [[CrossRef](#)]
44. Klatte, S.; Wendisch, V.F. Redox self-sufficient whole cell biotransformation for amination of alcohols. *Bioorganic Med. Chem.* **2014**, *22*, 5578–5585. [[CrossRef](#)] [[PubMed](#)]
45. Hennig, G.; Haupka, C.; Brito, L.F.; Rückert, C.; Cahoreau, E.; Heux, S.; Wendisch, V.F. Methanol-Essential Growth of *Corynebacterium glutamicum*: Adaptive Laboratory Evolution Overcomes Limitation due to Methanethiol Assimilation Pathway. *Int. J. Mol. Sci.* **2020**, *21*, 3617. [[CrossRef](#)] [[PubMed](#)]
46. Tuyishime, P.; Wang, Y.; Fan, L.; Zhang, Q.; Li, Q.; Zheng, P.; Sun, J.; Ma, Y. Engineering *Corynebacterium glutamicum* for methanol-dependent growth and glutamate production. *Metab. Eng.* **2018**, *49*, 220–231. [[CrossRef](#)] [[PubMed](#)]
47. Burkovski, A. Nitrogen Metabolism and Its Regulation. In *Handbook of Corynebacterium Glutamicum*; Eggeling, L., Bott, M., Eds.; CRC Press LLC: Boca Raton, FL, USA, 2005; pp. 335–352. ISBN 0-8493-1821-1.
48. Tesch, M.; Eikmanns, B.J.; de Graaf, A.A.; Sahm, H. Ammonia assimilation in *Corynebacterium glutamicum* and a glutamate dehydrogenase-deficient mutant. *Biotechnol. Lett.* **1998**, *20*, 953–957. [[CrossRef](#)]
49. Nolden, L.; Farwick, M.; Krämer, R.; Burkovski, A. Glutamine synthetases of *Corynebacterium glutamicum*: Transcriptional control and regulation of activity. *FEMS Microbiol. Lett.* **2001**, *201*, 91–98. [[CrossRef](#)] [[PubMed](#)]

50. Wendisch, V.F.; Lee, J.-H. Metabolic Engineering in *Corynebacterium glutamicum*. In *Corynebacterium Glutamicum*; Inui, M., Toyoda, K., Eds.; Microbiology Monographs; Springer International Publishing: Cham, Switzerland, 2020; Volume 23, pp. 287–322. ISBN 978-3-030-39266-6.
51. Arnold, F.H. Innovation by Evolution: Bringing New Chemistry to Life (Nobel Lecture). *Angew. Chem. Int. Ed.* **2019**, *58*, 14420–14426. [[CrossRef](#)]
52. Tenaillon, O.; Barrick, J.E.; Ribeck, N.; Deatherage, D.E.; Blanchard, J.L.; Dasgupta, A.; Wu, G.C.; Wielgoss, S.; Cruveiller, S.; Médigue, C.; et al. Tempo and mode of genome evolution in a 50,000-generation experiment. *Nature* **2016**, *536*, 165–170. [[CrossRef](#)]
53. Barrick, J.E.; Yu, D.S.; Yoon, S.H.; Jeong, H.; Oh, T.K.; Schneider, D.; Lenski, R.E.; Kim, J.F. Genome evolution and adaptation in a long-term experiment with *Escherichia coli*. *Nature* **2009**, *461*, 1243–1247. [[CrossRef](#)]
54. Dragosits, M.; Mattanovich, D. Adaptive laboratory evolution—Principles and applications for biotechnology. *Microb. Cell Factories* **2013**, *12*, 64. [[CrossRef](#)] [[PubMed](#)]
55. Wang, Y.; Fan, L.; Tuyishime, P.; Liu, J.; Zhang, K.; Gao, N.; Zhang, Z.; Ni, X.; Feng, J.; Yuan, Q.; et al. Adaptive laboratory evolution enhances methanol tolerance and conversion in engineered *Corynebacterium glutamicum*. *Commun. Biol.* **2020**, *3*. [[CrossRef](#)]
56. Leßmeier, L.; Wendisch, V.F. Identification of two mutations increasing the methanol tolerance of *Corynebacterium glutamicum*. *BMC Microbiol.* **2015**, *15*. [[CrossRef](#)]
57. Hanahan, D. Techniques for transformation of *E. coli*. *DNA Cloning Pract. Approach* **1985**, *1*, 109–135.
58. Eikmanns, B.J.; Thum-Schmitz, N.; Eggeling, L.; Lüdtkke, K.U.; Sahm, H. Nucleotide sequence, expression and transcriptional analysis of the *Corynebacterium glutamicum gltA* gene encoding citrate synthase. *Microbiology* **1994**, *140*, 1817–1828. [[CrossRef](#)]
59. Simon, R.; Priefer, U.; Pühler, A. A broad host range mobilization system for in vivo genetic engineering: Transposon mutagenesis in Gram negative bacteria. *BioTechnology* **1983**, *1*, 784–791. [[CrossRef](#)]
60. Gibson, D.G.; Young, L.; Chuang, R.-Y.; Venter, J.C.; Hutchison, C.A.; Smith, H.O. Enzymatic assembly of DNA molecules up to several hundred kilobases. *Nat. Methods* **2009**, *6*, 343–345. [[CrossRef](#)]
61. Schneider, J.; Niermann, K.; Wendisch, V.F. Production of the amino acids L-glutamate, L-lysine, L-ornithine and L-arginine from arabinose by recombinant *Corynebacterium glutamicum*. *J. Biotechnol.* **2011**, *154*, 191–198. [[CrossRef](#)]

